Inorganic Chemistry
Article

Inorg. Chem. **2010**, *49*, 7981–7991 **7981**
DOI: 10.1021/ic1009972

Synthesis and Solution Phase Characterization of Strongly Photooxidizing Heteroleptic Cr(III) Tris-Dipyridyl Complexes

Ashley M. McDaniel,[†,§] Huan-Wei Tseng,[‡,§] Niels H. Damrauer,*[,‡] and Matthew P. Shores*[,†]

[†]*Department of Chemistry, Colorado State University, Fort Collins, Colorado 80523-1872, and* [‡]*Department of Chemistry and Biochemistry, University of Colorado, Boulder, Colorado 80309-0215.* [§]*These authors contributed equally to this work.*

Received May 19, 2010

We report the preparation and characterization of Cr(III) coordination complexes featuring the dimethyl 2,2′-bipyridine-4,4′-dicarboxylate (4-dmcbpy) ligand: $[(phen)_2Cr(4\text{-}dmcbpy)](OTf)_3$ (**1**), $[(Ph_2phen)_2Cr(4\text{-}dmcbpy)](OTf)_3$ (**4**), $[(Me_2bpy)_2Cr(4\text{-}dmcbpy)](OTf)_3$ (**7**), and $[Cr(4\text{-}dmcbpy)_3](BF_4)_3$ (**8**), where phen is 1,10-phenanthroline, Ph_2phen is 4,7-diphenyl-1,10-phenanthroline, and Me_2bpy is 4,4′-dimethyl-2,2′-bipyridine. Static and nanosecond time-resolved absorption and emission properties of these complexes dissolved in acidic aqueous (1 M HCl) solutions are reported. Emission spectra collected at 297 K show a narrow spectrum with an emission maximum ranging from 732 nm (**1**) to 742 nm (**4**). The emissive state is thermally activated and decays via first order kinetics at all temperatures explored (283 to 353 K). At 297 K the observed lifetime ranges from 7.7 μs (**8**) to 108 μs (**4**). The photophysical data suggest that in these acidic aqueous environments these complexes store ~1.7 eV for multiple microseconds at room temperature. Of the heteroleptic species, complex **4** shows the greatest absorption of visible wavelengths (ε = 1270 M^{-1} cm^{-1} at 491 nm), and homoleptic complex **8** has improved absorption at visible wavelengths over $[Cr(bpy)_3]^{3+}$. The electrochemical properties of **1**, **4**, **7**, and **8** were investigated by cyclic voltammetry. It is found that inclusion of 4-dmcbpy shifts the "$Cr^{III/II}$" $E_{1/2}$ by +0.22 V compared to those of homoleptic parent complexes, with the first reduction event occurring at −0.26 V versus Fc^+/Fc for **8**. The electrochemical and photophysical data allow for excited state potentials to be determined: for **8**, $Cr^{III*/II}$ lies at +1.44 V versus ferrocenium/ferrocene (~+2 V vs NHE), placing it among the most powerful photooxidants reported.

Introduction

A large body of research has clarified the physical and synthetic prerequisites for achieving efficient light-to-electrical energy conversion in dye-sensitized solar cells (DSSCs) wherein excited states of inorganic chromophores can inject electrons into wide band gap semiconductors.[1−7] Early experimental successes, promising economic factors, and the sheer magnitude of the scientific issues involved have meant that other paradigms for dye-sensitization of charge transport remain relatively unexplored. One such opportunity involves photoinduced interfacial *hole* transfer. Optimization of this paradigm would expose numerous opportunities in solar energy conversion, including initiation of catalytic oxidative reactions critical for water splitting,[8−17] photocathodic solar cells (where current runs in the direction opposite to Grätzel cells),[18−21] and

*To whom correspondence should be addressed. E-mail: niels.damrauer@colorado.edu (N.H.D.), matthew.shores@colostate.edu (M.P.S.).

(1) O'Regan, B.; Grätzel, M. *Nature* **1991**, *353*, 737–740.
(2) Nazeeruddin, M. K.; Grätzel, M. In *Photofunctional Transition Metal Complexes*; Yam, V. W. W., Ed.; Springer: Berlin, 2007; pp 113−175.
(3) Robertson, N. *Angew. Chem., Int. Ed.* **2006**, *45*, 2338–2345.
(4) Polo, A. S.; Itokazu, M. K.; Iha, N. Y. M. *Coord. Chem. Rev.* **2004**, *248*, 1343–1361.
(5) Hagfeldt, A.; Grätzel, M. *Acc. Chem. Res.* **2000**, *33*, 269–277.
(6) Ardo, S.; Meyer, G. J. *Chem. Soc. Rev.* **2009**, *38*, 115–164.
(7) Martinson, A. B. F.; Hamann, T. W.; Pellin, M. J.; Hupp, J. T. *Chem.—Eur. J.* **2008**, *14*, 4458–4467.
(8) Gersten, S. W.; Samuels, G. J.; Meyer, T. J. *J. Am. Chem. Soc.* **1982**, *104*, 4029–4030.
(9) Lei, Y. B.; Hurst, J. K. *Inorg. Chim. Acta* **1994**, *226*, 179–185.
(10) Limburg, J.; Vrettos, J. S.; Liable-Sands, L. M.; Rheingold, A. L.; Crabtree, R. H.; Brudvig, G. W. *Science* **1999**, *283*, 1524–1527.
(11) Wada, T.; Tsuge, K.; Tanaka, K. *Angew. Chem., Int. Ed.* **2000**, *39*, 1479–1482.
(12) Sens, C.; Romero, I.; Rodriguez, M.; Llobet, A.; Parella, T.; Benet-Buchholz, J. *J. Am. Chem. Soc.* **2004**, *126*, 7798–7799.
(13) Zong, R.; Thummel, R. P. *J. Am. Chem. Soc.* **2005**, *127*, 12802–12803.
(14) Tseng, H.-W.; Zong, R.; Muckerman, J. T.; Thummel, R. *Inorg. Chem.* **2008**, *47*, 11763–11773.
(15) Kanan, M. W.; Nocera, D. G. *Science* **2008**, *321*, 1072–1075.
(16) McDaniel, N. D.; Coughlin, F. J.; Tinker, L. L.; Bernhard, S. *J. Am. Chem. Soc.* **2008**, *130*, 210–217.
(17) Eisenberg, R.; Gray, H. B. *Inorg. Chem.* **2008**, *47*, 1697–1699, and papers published in the forum.
(18) Morandeira, A.; Boschloo, G.; Hagfeldt, A.; Hammarström, L. *J. Phys. Chem. C* **2008**, *112*, 9530–9537.
(19) Qin, P.; Wiberg, J.; Gibson, E. A.; Linder, M.; Li, L.; Brinck, T.; Hagfeldt, A.; Albinsson, B.; Sun, L. *J. Phys. Chem. C* **2010**, *114*, 4738–4748.
(20) Qin, P.; Linder, M.; Brinck, T.; Boschloo, G.; Hagfeldt, A.; Sun, L. *Adv. Mater.* **2009**, *21*, 2993–2996.

© 2010 American Chemical Society
Published on Web 08/09/2010

tandem photovoltaic cells,[22−24] where both electrodes are photoactive.[25]

Despite these promises, relatively little is known about the physio-chemical factors that must be controlled if photoinduced hole injection processes are to be exploited for solar energy conversion. To our knowledge, there are only a few reports in the literature where this initial photophysical mechanism drives a photocathodic current in a DSSC device.[21,28−31] There are only three systems reported where hole injection is time-resolved and shown to be ultrafast[18,32,33] and only three disclosures where hole transfer participates in a dye-sensitized heterojunction solar cell.[34−36] Finally, only in three reports has hole injection functioned as one-half of a tandem photovoltaic cell.[23,37,38] The latter of these is the current efficiency record holder for *p*-type DSSCs (0.20% overall efficiency). Clearly, whereas the paucity of results alludes to the significant challenges involved in this area, it also offers the freedom to explore new materials and methods for controlling energetics and carrier-transfer rates.

Searching for molecular sensitizers capable of initiating excited-state oxidation of wide band gap semiconductors, we note tris-dipyridyl complexes of Cr(III) as one promising class of compounds. Serpone and Hoffman studied homoleptic analogues for solar energy conversion purposes about 25 years ago.[39−45] Parent complexes such as $[Cr(bpy)_3]^{3+}$ or $[Cr(phen)_3]^{3+}$ have excited state redox potentials sufficient to oxidize water to dioxygen if $4e^-$ oxidation could be achieved. They also have long excited state lifetimes, which should promote hole injection into an attached semiconductor surface. Although they absorb visible light ~50 times more weakly than $[Ru(bpy)_3]^{2+}$ (at 450 nm),[39,46] chromium is several orders of magnitude more abundant than ruthenium,[47] and ligand modifications can improve absorption properties (vide infra).

Scheme 1. Target Structures of $[(NN)_2Cr(4\text{-dmcbpy})]^{3+}$ Complexes[a]

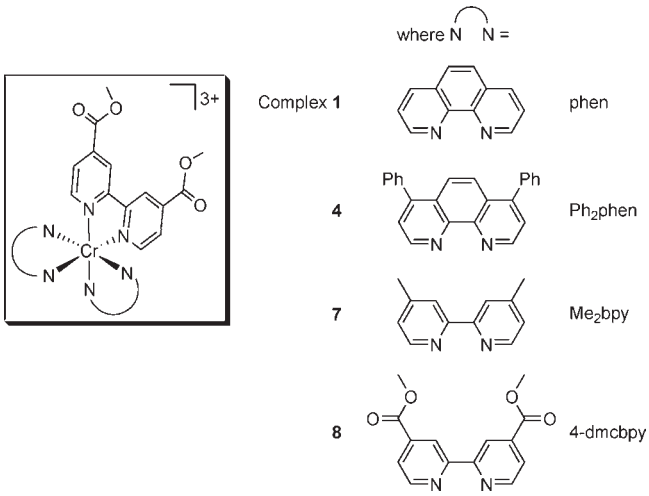

[a] The (NN) ligands impart electronic tunability, while 4-dmcbpy makes possible covalent attachment to semiconductor surfaces.

Heteroleptic polypyridyl complexes of Cr(III) represent potentially functional model systems, which to our knowledge have not been studied as components of hybrid materials. Dipyridyl ligands with carboxylate functional groups located at the 4 and 4′ positions can serve to anchor the sensitizer to metal oxide surfaces, as has been demonstrated extensively in Ru(II)-containing analogues.[1−7] As discussed in this paper, the electronic properties of the Cr(III) center can be tuned by judicious choice of the ancillary dipyridyl-type ligands (NN). Although structurally homologous with Ru(II) complexes, the synthesis of heteroleptic Cr(III) dipyridyl complexes is not straightforward, as efforts to activate the inert metal center often result in ligand scrambling.[48] Nevertheless, a recently disclosed methodology employing $[(NN)_2Cr(OTf)_2]^+$ complexes as synthons[48−50] shows the way to a new class of molecular species with potential for efficient hole injection into semiconductor substrates. Herein, we describe the preparations as well as electrochemical and photophysical investigations of a family of structurally related heteroleptic Cr(III) dipyridyl complexes (Scheme 1). The solution phase investigation of these compounds demonstrates their

(21) Qin, P.; Zhu, H.; Edvinsson, T.; Boschloo, G.; Hagfeldt, A.; Sun, L. *J. Am. Chem. Soc.* **2008**, *130*, 8570–8571.
(22) Nattestad, A.; Mozer, A. J.; Fischer, M. K. R.; Cheng, Y. B.; Mishra, A.; Bauerle, P.; Bach, U. *Nat. Mater.* **2010**, *9*, 31–35.
(23) He, J.; Lindström, H.; Hagfeldt, A.; Lindquist, S.-E. *Sol. Energy Mater. Sol. Cells* **2000**, *62*, 265–273.
(24) Mizoguchi, Y.; Fujihara, S. *Electrochem. Solid-State Lett.* **2008**, *11*, K78–K80.
(25) The theoretical efficiency limit for third generation[26] photovoltaic tandem cells, where each of the chromophores absorbs a different portion of the solar spectrum, is ~45%.[23,27] This compares favorably to the maximum ~30% efficiency achievable in Grätzel-type cells operating with one active electrode.
(26) Green, M. *Third Generation Photovoltaics: Advanced Solar Energy Conversion*; Springer-Verlag: Berlin, 2003.
(27) Hanna, M. C.; Nozik, A. J. *J. Appl. Phys.* **2006**, *100*, 074510–074518.
(28) Nattestad, A.; Ferguson, M.; Kerr, R.; Cheng, Y.-B.; Bach, U. *Nanotechnology* **2008**, *19*, 295304.
(29) Mori, S.; Fukuda, S.; Sumikura, S.; Takeda, Y.; Tamaki, Y.; Suzuki, E.; Abe, T. *J. Phys. Chem. C* **2008**, *112*, 16134–16139.
(30) Borgström, M.; Blart, E.; Boschloo, G.; Mukhtar, E.; Hagfeldt, A.; Hammarström, L.; Odobel, F. *J. Phys. Chem. B* **2005**, *109*, 22928–22934.
(31) Odobel, F.; Le Pleux, L.; Pellegrin, Y.; Blart, E. *Acc. Chem. Res.* DOI: 10.1021/ar900275b.
(32) Morandeira, A.; Edvinsson, T.; Le Pleux, L.; Blart, E.; Boschloo, G.; Hagfeldt, A.; Hammarström, L.; Odobel, F. *J. Phys. Chem. C* **2008**, *112*, 1721–1728.
(33) Morandeira, A.; Boschloo, G.; Hagfeldt, A.; Hammarström, L. *J. Phys. Chem. B* **2005**, *109*, 19403–19410.
(34) O'Regan, B.; Schwartz, D. T. *J. Appl. Phys.* **1996**, *80*, 4749–4754.
(35) O'Regan, B.; Lenzmann, F.; Muis, R.; Wienke, J. *Chem. Mater.* **2002**, *14*, 5023–5029.
(36) Rusop, M.; Soga, T.; Jimbo, T.; Umeno, M. *Surf. Rev. Lett.* **2004**, *11*, 577–583.
(37) Nakasa, A.; Usami, H.; Sumikura, S.; Hasegawa, S.; Koyama, T.; Suzuki, E. *Chem. Lett.* **2005**, *34*, 500–501.
(38) Gibson, E. A.; Smeigh, A. L.; Le Pleux, L.; Fortage, J.; Boschloo, G.; Blart, E.; Pellegrin, Y.; Odobel, F.; Hagfeldt, A.; Hammarström, L. *Angew. Chem., Int. Ed.* **2009**, *48*, 4402–4405.
(39) Serpone, N.; Jamieson, M. A.; Henry, M. S.; Hoffman, M. Z.; Bolletta, F.; Maestri, M. *J. Am. Chem. Soc.* **1979**, *101*, 2907–2916.
(40) Serpone, N.; Jamieson, M. A.; Emmi, S. S.; Fuochi, P. G.; Mulazzani, Q. G.; Hoffman, M. Z. *J. Am. Chem. Soc.* **1981**, *103*, 1091–1098.
(41) Serpone, N.; Jamieson, M. A.; Sriram, R.; Hoffman, M. Z. *Inorg. Chem.* **1981**, *20*, 3983–3988.
(42) Hoffman, M. Z.; Serpone, N. *Isr. J. Chem.* **1982**, *22*, 91–97.
(43) Bolletta, F.; Maestri, M.; Moggi, L.; Jamieson, M. A.; Serpone, N.; Henry, M. S.; Hoffman, M. Z. *Inorg. Chem.* **1983**, *22*, 2502–2509.
(44) Serpone, N.; Hoffman, M. Z. *J. Chem. Educ.* **1983**, *60*, 853–860.
(45) Jamieson, M. A.; Serpone, N.; Hoffman, M. Z. *Coord. Chem. Rev.* **1981**, *39*, 121–179.
(46) Juris, A.; Balzani, V.; Barigelletti, F.; Campagna, S.; Belser, P.; Vonzelewsky, A. *Coord. Chem. Rev.* **1988**, *84*, 85–277.
(47) Greenwood, N. N.; Earnshaw, A. *Chemistry of the Elements*, 2nd ed.; Elsevier Butterworth-Heinemann: Oxford, 1997.
(48) Barker, K. D.; Barnett, K. A.; Connell, S. M.; Glaeser, J. W.; Wallace, A. J.; Wildsmith, J.; Herbert, B. J.; Wheeler, J. F.; Kane-Maguire, N. A. P. *Inorg. Chim. Acta* **2001**, *316*, 41–49.
(49) Isaacs, M.; Sykes, A.; Ronco, S. *Inorg. Chim. Acta* **2006**, *359*, 3847–3854.
(50) Donnay, E. G.; Schaeper, J. P.; Brooksbank, R. D.; Fox, J. L.; Potts, R. G.; Davidson, R. M.; Wheeler, J. F.; Kane-Maguire, N. A. P. *Inorg. Chim. Acta* **2007**, *360*, 3272–3280.

ability to act as strong photooxidants, and the electronic flexibility afforded by ligand substitution allows us to explore fundamental structure/function relationships in our search for efficient hole transfer to semiconductor substrates.

Experimental Section

Preparation of Compounds. Unless otherwise noted, the syntheses of heteroleptic tris-dipyridyl Cr(III) complexes were performed in air with atmospheric moisture excluded by use of a $CaCO_3$-filled drying tube. For synthetic routes employing Cr(II) starting materials and for the preparation of $[Cr(NN)_2(OTf)_2]OTf$ (OTf = trifluoromethanesulfonate), compound manipulations were performed either inside a dinitrogen-filled glovebox (MBRAUN Labmaster 130) or via Schlenk techniques on an inert gas (N_2) manifold. The commercially obtained ligand 4,4′-dimethyl-2,2′-bipyridine (Me_2bpy) was recrystallized from ethyl acetate before use. The ligand dimethyl 2,2′-bipyridine-4,4′-dicarboxylate (4-dmcbpy) was synthesized according to the literature.[51] The preparations of $[(phen)_2Cr(OTf)_2](OTf)$, $[(bpy)_2Cr(OTf)_2](OTf)$, and $[Cr(CH_3CN)_4(BF_4)_2]$ have been described elsewhere.[52,53] The homoleptic complexes $[Cr(NN)_3](OTF)_3$, where (NN) is phen, Ph_2phen, or Me_2bpy, were prepared by refluxing $[Cr(NN)_2(OTf)_2]OTf$ in CH_2Cl_2, with 5 equiv of the same (NN) ligand for 16 h and collecting the precipitated yellow solids by filtration. The complex $[Cr(bpy)_3](BF_4)_3$ was prepared analogously to $[Cr(4\text{-dmcbpy})_3](BF_4)_3$ (**8**),[39] using bpy in place of 4-dmcbpy. Electronic absorption spectra, electrospray ionization mass spectrometry (ESI-MS), and clean electrochemical traces confirmed the identity and purity of the previously reported homoleptic complexes. Pentane was distilled over sodium metal and subjected to three freeze−pump−thaw cycles. Other solvents were sparged with dinitrogen, passed over alumina, and degassed prior to use. All other reagents were obtained from commercial sources and were used without further purification.

$[(phen)_2Cr(4\text{-dmcbpy})](OTf)_3$ (1). Solid 4-dmcbpy (0.71 g, 2.62 mmol) was added to a solution of $[(phen)_2Cr(OTf)_2]OTf$ (1.50 g, 1.75 mmol) in 125 mL of dichloromethane and heated to reflux. Over 5 days, a bright yellow precipitate formed. The solid was isolated by filtration, washed with dichloromethane (3 × 30 mL), and dried in vacuo to afford 1.86 g (94%) of product. IR (KBr pellet): $\nu_{C=O}$ 1728 cm^{-1}. μ_{eff} (295 K): 3.90 μ_B. ES^+MS (CH_3CN): m/z 228.27 ($[\mathbf{1} - 3OTf]^{3+}$), 981.67 ($[\mathbf{1} - OTf]^+$). Anal. Calcd. for $C_{41}H_{28}N_6CrF_9O_{13}S_3$: C, 43.51; H, 2.49; N, 7.42. Found: C, 43.23; H, 2.33; N, 7.27. Crystals suitable for X-ray analysis were obtained by slow diffusion of diethyl ether into an acetonitrile solution of the compound.

$[(Ph_2phen)_2CrCl_2]Cl$ (2). Solid anhydrous $CrCl_3$ (0.10 g, 0.60 mmol) was added to a suspension of Ph_2phen (0.40 g, 1.20 mmol) in 35 mL of absolute ethanol. A trace amount (< 2 mg) of zinc dust was added, and the mixture was heated to reflux for 1 h, resulting in a green-brown mixture. The mixture was filtered, and an olive green solid was isolated from the filtrate by rotary evaporation to afford 0.49 g (98%) of product. IR (KBr pellet): $\nu_{C=N}$ 1620 cm^{-1}. ES^+MS (CH_3CN): m/z 788.27 ($[\mathbf{2} - Cl]^+$). The compound was used in the next synthetic step without further purification or characterization.

$[(Ph_2phen)_2Cr(OTf)_2]OTf$ (3). Under a dinitrogen atmosphere, trifluoromethanesulfonic acid (2 mL, 22.60 mmol) was slowly added to solid **2** (0.40 g, 0.49 mmol) to give a red-orange solution. Dinitrogen was bubbled through the stirring solution for 24 h, after which the solution was cooled in an ice bath and 250 mL of diethyl ether was added. After standing 4 h, a beige-peach colored solid precipitated from solution. The solid was isolated by vacuum filtration and rinsed with diethyl ether (3 × 30 mL) to afford 0.47 g (83%) of product. IR (KBr pellet): $\nu_{C=N}$ 1625 cm^{-1}. ES^+MS (CH_3CN): m/z 1014.20 ($[\mathbf{3} - OTf]^+$). The compound was used in the next synthetic step without further purification or characterization.

$[(Ph_2phen)_2Cr(4\text{-dmcbpy})](OTf)_3$ (4). Solid 4-dmcbpy (0.140 g, 0.515 mmol) was added to a solution of **3** (0.209 g, 0.17 mmol) in 30 mL of dichloromethane and heated to reflux. Over 14 days, a yellow precipitate formed. The solid was isolated by filtration, washed with dichloromethane (3 × 10 mL) and collected to afford 0.07 g (27%) of product. IR (KBr pellet): $\nu_{C=O}$ 1734 cm^{-1}. μ_{eff} (295 K): 3.36 μ_B. ES^+MS (CH_3CN): m/z 329.80 ($[\mathbf{4} - 3OTf]^{3+}$), 1285.60 ($[\mathbf{4} - OTf]^+$). Anal. Calcd. for $C_{65}H_{44}N_6CrF_9O_{13}S_3$: C, 54.36; H, 3.09; N, 5.85. Found: C, 54.12; H, 3.05; N, 5.75.

$[(Me_2bpy)_2CrCl_2]Cl$ (5). Solid anhydrous $CrCl_3$ (0.43 g, 2.71 mmol) was added to a solution of Me_2bpy (1.00 g, 5.43 mmol) in 60 mL of absolute ethanol. A trace amount (< 4 mg) of zinc dust was added, and the mixture heated to reflux for 1 h, resulting in a green-brown solution. A gray-green solid precipitated from the reaction mixture upon cooling. It was collected by filtration, washed with cold absolute ethanol (3 × 10 mL), and dried in vacuo to afford 1.12 g (78%) of product. IR (KBr pellet): $\nu_{C=N}$ 1616 cm^{-1}. ES^+MS (CH_3CN): m/z 490.00 ($[\mathbf{5} - Cl]^+$). The compound was used in the next synthetic step without further purification or characterization.

$[(Me_2bpy)_2Cr(OTf)_2]OTf$ (6). Under a dinitrogen atmosphere, trifluoromethanesulfonic acid (2 mL, 22.60 mmol) was added to solid **5** (0.35 g, 0.67 mmol) to give a red-orange solution. Dinitrogen was bubbled through the stirring solution for 24 h, after which the solution was cooled in an ice bath. Diethyl ether (250 mL) was slowly added to form a pink precipitate. The solid was isolated by filtration and rinsed with diethyl ether (3 × 50 mL) to afford 0.53 g (92%) of product. IR (KBr pellet): $\nu_{C=N}$ 1627 cm^{-1}. ES^+MS (CH_3CN): m/z 718.13 ($[\mathbf{6} - OTf]^+$). The compound was used in the next synthetic step without further purification or characterization.

$[(Me_2bpy)_2Cr(4\text{-dmcbpy})](OTf)_3$ (7). Solid 4-dmcbpy (0.07 g, 0.26 mmol) was added to a solution of **6** (0.20 g, 0.23 mmol) in 30 mL of dichloromethane and heated to reflux. Over 9 days, a light yellow precipitate was formed. The solid was isolated by filtration, washed with dichloromethane (3 × 10 mL) and dried in vacuo to afford 0.13 g (48%) of product. IR (KBr pellet): $\nu_{C=O}$ 1739 cm^{-1}. μ_{eff} (295 K): 4.01 μ_B. ES+MS (CH_3CN): m/z 230.93 ($[\mathbf{7} - 3OTf]^{3+}$), 989.60 ($[\mathbf{7} - OTf]^+$). Anal. Calcd. for $C_{41}H_{36}N_6CrF_9O_{13}S_3$: C, 43.20; H, 3.18; N, 7.37. Found: C, 42.94; H, 3.11; N, 7.28.

$[Cr(4\text{-dmcbpy})_3](BF_4)_3$ (8). Under a dinitrogen atmosphere, a solution of $[Cr(CH_3CN)_4(BF_4)_2]$ (0.13 g, 0.74 mmol) in 4 mL of acetonitrile was added to a suspension of 4-dmcbpy (0.33 g, 2.44 mmol) in 4 mL of acetonitrile to form a forest green solution. The solvent was removed in vacuo to afford a forest green solid. Addition of $AgBF_4$ (0.04 g, 0.19 mmol) to a solution of the isolated green solid (0.20 g, 0.19 mmol) in 5 mL of acetonitrile resulted in a yellow solution along with a light gray solid. The solution was filtered, and the filtrate was treated with 15 mL of diethyl ether to precipitate a bright yellow solid. The solid was recrystallized by diethyl ether diffusion into acetonitrile resulting in bright yellow crystals. The crystals were collected by filtration, washed with dichloromethane (3 × 3 mL) followed by diethyl ether (3 × 5 mL) and dried in vacuo to afford 0.10 g (45%) of product. IR (mineral oil): $\nu_{C=O}$ 1737 cm^{-1}. μ_{eff} (295 K): 4.15 μ_B. ES^+MS (CH_3CN): m/z 289.67 ($[\mathbf{8} - 3BF_4]^{3+}$). Anal. Calcd. for $C_{42}H_{36}N_6CrF_{12}B_3O_{12}$: C, 44.67; H, 3.21; N, 7.44. Found: C, 44.46; H, 3.08; N, 7.28.

X-ray Structure Determination. A suitable crystal of **1**·1.3CH_3CN was coated with Paratone-N oil and supported on a Cryoloop before being mounted on a Bruker Kappa Apex II CCD diffractometer under a stream of dinitrogen. Data collection was performed at 110 K with Mo Kα radiation and a graphite monochromator. Crystallographic data and metric parameters are presented in Table 1. Data were integrated and

(51) Garelli, N.; Vierling, P. *J. Org. Chem.* **1992**, *16*, 3046–3051.
(52) Ryu, C. K.; Endicott, J. F. *Inorg. Chem.* **1988**, *27*, 2203–2214.
(53) Henriques, R. T.; Herdtweck, E.; Kuhn, F. E.; Lopes, A. D.; Mink, J.; Romao, C. C. *J. Chem. Soc., Dalton Trans.* **1998**, 1293–1297.

Table 1. Crystallographic Data[a] for $[(phen)_2Cr(4\text{-}dmcbpy)](OTf)_3 \cdot 1.3CH_3CN$ ($\mathbf{1} \cdot 1.3CH_3CN$)

	$\mathbf{1} \cdot 1.3CH_3CN$
formula	$C_{43.60}H_{31.90}CrF_9N_{7.30}O_{13}S_3S_3$
formula wt	1185.24
color, habit	yellow plates
T, K	110(2)
space group	$P\bar{1}$ (triclinic)
Z	2
a, Å	12.6215(7)
b, Å	13.9620(8)
c, Å	17.2034(15)
α, deg	99.574(4)
β, deg	106.338(4)
γ, deg	115.479(2)
V, Å^3	2477.6(3)
d_{calc}, g/cm^3	1.589
GOF	1.026
R_1 (wR_2)[b], %	4.64 (10.17)

[a] Obtained with graphite-monochromated Mo K_α (λ = 0.71073 Å) radiation. [b] $R_1 = \sum||F_o| - |F_c||/\sum|F_o|$, $wR_2 = \{\sum w(F_o^2 - F_c^2)^2/\sum w(F_o^2)^2\}^{1/2}$ for $F_o > 4\sigma(F_o)$.

corrected for Lorentz and polarization effects using SAINT, and semiempirical absorption corrections were applied using SADABS.[54] The structure was solved by direct methods and refined against F^2 with the SHELXTL 6.14 software package.[55] Unless otherwise noted, thermal parameters for all non-hydrogen atoms were refined anisotropically. Hydrogen atoms were added at the ideal positions and were refined using a riding model where the thermal parameters were set at 1.2 times those of the attached carbon atom (1.5 for methyl protons). In the structure of $\mathbf{1} \cdot 1.3CH_3CN$, two of the triflate anions show positional disorder, and one solvent molecule is only partially occupied. Complete experimental parameters and disorder treatment are discussed in the Supporting Information.

Photophysical Measurements. All photophysical measurements were undertaken with complexes dissolved in 1 M $HCl_{(aq)}$. This alters the nucleophilicity of the solvent, thereby decreasing the quantum yield of associative excited state reactions (formation of seven-coordinate solvento species) which ultimately would lead to polypyridyl ligand substitution by solvent molecules.[39,56,57] The ground-state absorption spectra were obtained with a Hewlett-Packard 8453 spectrophotometer in quartz cuvettes with 1 cm or 1 mm path lengths; experiments were performed at room temperature. Quartz cuvettes (1 cm ×1 cm) with silicone septa seal screw caps were used for the following measurements. Transient absorption spectra were obtained at 20−21 °C without deoxygenation (see Supporting Information for details). Emission spectra, emission quantum yields, and single-temperature emission lifetime experiments were measured at 23−24 °C with deoxygenation on dilute samples (see Supporting Information for details). Teflon tubing was used to introduce a stream of argon into the solution. Prior to measurements, samples were purged with argon for 30 min to remove oxygen. For the longer lifetime species such as $[Cr(phen)_3]^{3+}$, which are highly sensitive to $^3O_2$ concentrations, this methodology proved easier and far more effective at achieving reproducible results than using freeze−pump−thaw cycles. Each measurement was done with argon flowing on top of the solution. In these emission experiments the temperature of the sample was controlled using a water-jacket cuvette holder connected to a constant-temperature circulator. For temperature-dependent experiments, emission lifetimes were measured every 10 °C from 10 to 80 °C, and the lifetime measured at 23−24 °C was also included.

For the normalized emission quantum yields reported in Table 3, we compared the integrated emission of each complex relative to that of the standard $[Cr(phen)_3]^{3+}$ in 1 M $HCl_{(aq)}$ according to the eq 1.[58] Both measurements are made back to back.

$$\Phi_{unk} = \Phi_{std}\left(\frac{I_{unk}}{A_{unk}}\right)\left(\frac{A_{std}}{I_{std}}\right)\left(\frac{\eta_{unk}}{\eta_{std}}\right)^2 \quad (1)$$

In this expression, Φ_{unk} and Φ_{std} are the emission quantum yields of the unknown and standard, respectively, under the conditions of the measurement. To our knowledge Φ_{std} (for $[Cr(phen)_3]^{3+}$) has not been previously measured and is set to *one* in this column of Table 3 as has been done previously.[39,57] The quantities I_{unk} and I_{std} are the integrated emission intensities of the sample and the standard, respectively, at 650−850 nm. The quantities A_{unk} and A_{std} are the absorbances of the sample and the standard, respectively, at the excitation wavelength (320 nm). Care was taken to ensure that these are both close to 0.1. Finally η_{unk} and η_{std} are the indices of refraction of the sample and the standard solution, respectively. Since the same solvent was used in both measurements, the last term in eq 1 can be ignored. For these measurements, no differences were observed in absorption spectra collected before and after the emission measurements.

To determine the emission quantum yields reported in Table 3, we first measured Φ_{unk} for $[Cr(phen)_3](OTF)_3$ in 1 M $HCl_{(aq)}$ relative to $[Ru(bpy)_3](PF_6)_2$ in acetonitrile for which the absolute quantum yield (Φ_{std}) of 0.062 is known.[59] The refractive indices of pure acetonitrile and 1 M $HCl_{(aq)}$ were used in the calculation. The quantum yields for the rest of the seven complexes were then calculated with respect to Φ_{unk} determined for $[Cr(phen)_3]^{3+}$. The error bars reported with these seven quantum yields are determined by combining the percentage experimental errors from the individual normalized emission quantum yields (A%) with the percentage error in the measurement made between $[Cr(phen)_3]^{3+}$ and $[Ru(bpy)_3]^{2+}$ (B%) according to the equation $Error\% = (A^2 + B^2)^{1/2}\%$.

Further detailed information about instrumentation and methods for photophysical measurements are included in the Supporting Information.

Other Physical Methods. Infrared spectra were measured with a Nicolet 380 FT-IR spectrometer. Mass spectrometric measurements were performed in the positive ion mode on a Finnigan LCQ Duo mass spectrometer, equipped with an analytical electrospray ion source and a quadrupole ion trap mass analyzer. Cyclic voltammetry experiments were carried out inside a dinitrogen filled glovebox in 0.1 M solutions of $(Bu_4N)PF_6$ in acetonitrile unless otherwise noted. The voltammograms were recorded with either a CH Instruments 1230A or 660C potentiostat using a 0.25 mm Pt disk working electrode, Ag wire quasi-reference electrode, and at a Pt mesh auxiliary electrode. All voltammograms shown were measured with a scan rate of 0.1 V/s. Reported potentials are referenced to the ferrocenium/ferrocene (Fc^+/Fc) redox couple and were determined by adding ferrocene as an internal standard at the conclusion of each electrochemical experiment. Solid state magnetic susceptibility measurements were performed on finely ground samples prepared in air using a Quantum Design model MPMS-XL SQUID magnetometer at 295 K. The data were corrected for the magnetization of the sample holder by subtracting the susceptibility of an empty container; diamagnetic corrections were applied using Pascal's constants.[60] Elemental analyses were performed by Robertson Microlit Laboratories, Inc. in Madison, NJ.

(54) *APEX 2*; Bruker Analytical X-Ray Systems, Inc.: Madison, WI, 2008.
(55) Sheldrick, G. M. *SHELXTL*, Version 6.14; Bruker Analytical X-Ray Systems, Inc.: Madison, WI, 1999.
(56) Kalyanasundaram, K. *Photochemistry of Polypyridine and Porphyrin Complexes*; Academic Press: London, 1992.
(57) Brunschwig, B.; Sutin, N. *J. Am. Chem. Soc.* **1978**, *100*, 7568–7577.
(58) Demas, J. N.; Crosby, G. A. *J. Phys. Chem.* **1971**, *75*, 991–1024.
(59) Calvert, J. M.; Caspar, J. V.; Binstead, R. A.; Westmoreland, T. D.; Meyer, T. J. *J. Am. Chem. Soc.* **1982**, *104*, 6620–6627.
(60) Bain, G. A.; Berry, J. F. *J. Chem. Educ.* **2008**, *85*, 532–536.

Scheme 2

$$[(NN)_2CrCl_2]Cl \xrightarrow[-3HCl]{\text{xs HOTf}} [(NN)_2Cr(OTf)_2](OTf) \xrightarrow[CH_2Cl_2]{\text{4-dmcbpy}} [(NN)_2Cr(4\text{-dmcbpy})](OTf)_3$$

Scheme 3

$$[Cr(CH_3CN)_4(BF_4)_2] \xrightarrow[CH_3CN,\ N_2]{\text{3 (4-dmcbpy)}} [Cr(4\text{-dmcbpy})_3](BF_4)_2 \xrightarrow[CH_3CN]{AgBF_4} Ag + [Cr(4\text{-dmcbpy})_3](BF_4)_3$$

Results and Discussion

Synthesis and Characterization of Heteroleptic Cr(III) Complexes. Although there is literature precedent for heteroleptic Cr(III) dipyridyl complexes, the preparation of species that contain at least one carboxylate group (for eventual attachment to semiconductor surfaces) was not known prior to our efforts. The preparative routes we have developed are outlined in Schemes 2−3. Typically, heteroleptic dipyridyl complexes of Cr(III) are synthesized using $[(NN)_2Cr(OTf)_2](OTf)$ precursors: the weakly coordinating triflate anions can be facilely removed from otherwise inert Cr(III) centers, and replaced by a third diimine species with minimal ligand scrambling.[48−50] Initial attempts to prepare complexes using 2,2′-bipyridine-4,4′-dicarboxylic acid (dcbpy) or its disodium salt do not afford pure products. Whereas mass spectral analyses show peaks at anticipated m/z ratios (consistent with $[(phen)_2Cr(4\text{-dcbpy})]^+$), analysis of isotopic distribution patterns reveal 2+ charges for those ions. We speculate that the products actually formed are dimeric $[(NN)_2Cr(4\text{-dcbpy})]_2^{2+}$ species, where carboxylates coordinate in preference to the imines because of the oxophilic nature of Cr(III), allowing the 4-dcbpy ligand to bridge between two metal centers. Masking the carboxylates on dcbpy by conversion to methyl ester groups (4-dmcbpy) avoids undesirable metal coordination by the carboxylates. Where (NN) is phen, Ph_2phen, or Me_2bpy, the ester-protected ligand 4-dmcbpy is found to react cleanly, albeit sluggishly, with $[(NN)_2Cr(OTf)_2](OTf)$ via Scheme 2 to form the heteroleptic complexes **1**, **4**, and **7**, respectively, as yellow solids.

The homoleptic complex salt $[Cr(4\text{-dmcbpy})_3](OTf)_3$ (**8**) cannot be prepared via Scheme 2, since deprotection of the esters during triflate exchange with $[Cr(4\text{-dmcbpy})_2Cl_2]Cl$ results in dimerization of the Cr complexes. Instead, we find that a Cr(II) solvento complex, $[Cr(CH_3CN)_4(BF_4)_2]$, can serve as a suitable starting material.[53] The labile Cr(II) ion is easily ligated by 3 equiv of the 4-dmcbpy ligand. Oxidation by Ag(I) affords the tetrafluoroborate salt of the homoleptic Cr(III) complex in reasonable yield (Scheme 3).

In contrast to the phen-containing heteroleptic complex **1**, the bpy-containing analogue $[(bpy)_2Cr(4\text{-dmcbpy})]^{3+}$ resists formation via Scheme 2, although the reasons for this are not known at this time. To our knowledge, only two successful syntheses of bpy-containing heteroleptic complexes have been reported, $[(bpy)_2Cr(phen)](OTf)_3$[48] and $[(bpy)_2Cr(DPPZ)](OTf)_3$ (where DPPZ is dipyridophenazine).[61] We speculate that the ring-locked configuration and higher basicity of the phenanthroline-type ligands minimize opportunities for deleterious ligand exchange before replacement of the more labile triflate anions, whereas the less rigid dipyridyl ligands offer greater opportunity for ligand scrambling. Attempts to make heteroleptic bpy-containing complexes via the more reactive Cr(II) synthon (Scheme 3) have led thus far to intractable mixtures of homo- and heteroleptic products.

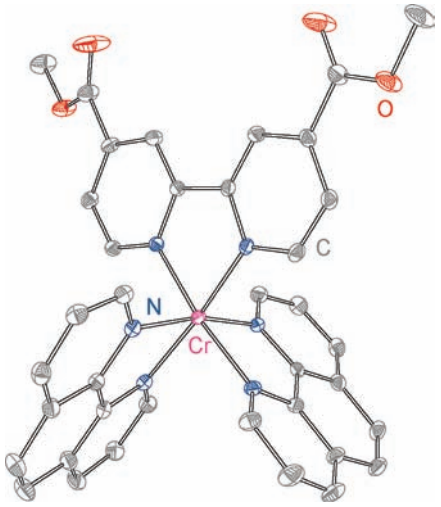

Figure 1. Structure of the $[(phen)_2Cr(4\text{-dmcbpy})]^{3+}$ complex cation, as observed in $\mathbf{1}\cdot 1.3CH_3CN$, rendered with 40% ellipsoids. H atoms are omitted for clarity. The complex resides on a general position. Bond distances and angles are available in the Supporting Information.

Besides the usual methods employed for identification and characterization of the complexes, the solid state structure of the phen-containing complex **1** has been confirmed by X-ray crystallography (Figure 1). All bond distances and angles are as expected for a Cr(III) ion in a tris-chelate ligand environment. Relevant crystallographic data are shown in Table 1; additional structural and geometric data are included in the Supporting Information.

Exploration of Photophysics and Electrochemistry of Cr(III) Systems in Solution. We have explored the basic photophysical and electrochemical properties of these systems to better understand the nascent and long-lived excited-states that will be called upon to drive hole-injection following photoexcitation in later studies. Key questions to be addressed here include: (1) how efficient are these complexes as optical absorbers; (2) how much energy is stored in the excited state; (3) for how long is it stored in unbound solution phase systems; (4) with what driving force might we expect hole transfer photochemistry; and (5) what are the transient absorption features we might use in later femtosecond pump/probe studies to determine hole-injection rates.

Electronic Absorption. Sensitization of hole transfer photochemistry demands light absorption in the material-bound metal complex as an initial step. If Cr(III) polypyridyl complexes are to serve in this role it is important that ligand modifications render visible light absorption more efficient than pure spin-allowed ligand-field excitation ($\varepsilon = 50-100\ M^{-1}\ cm^{-1}$). UV−visible absorption spectra in 1 M $HCl_{(aq)}$ for complexes containing substituted bipyridine ligands are shown in Figure 2. Also included for purposes of comparison are spectra for $[Cr(bpy)_3]^{3+}$ and $[Cr(Me_2bpy)_3]^{3+}$. Absorption data for all complexes considered in this manuscript are presented in Table 2. Note that spectra for previously reported homoleptic complexes[39] were reacquired to allow for unambiguous quantitative comparisons to the new heteroleptic complexes.

(61) Vandiver, M. S.; Bridges, E. P.; Koon, R. L.; Kinnaird, A. N.; Glaeser, J. W.; Campbell, J. F.; Priedemann, C. J.; Rosenblatt, W. T.; Herbert, B. J.; Wheeler, S. K.; Wheeler, J. F.; Kane-Maguire, N. A. P. *Inorg. Chem.* **2010**, *49*, 839–848.

Table 2. Room Temperature Electronic Absorptions for Cr(III) Tris-Dipyridyl Complexes

complex	λ_{max}/nm (ε/M^{-1} cm^{-1})
$[Cr(phen)_3](OTf)_3$	269 (52500); 285 (31800), sh; 323 (11200), sh; 342 (6810), sh; 358 (3710); 405 (821), sh; 435 (558), sh; 454 (285), sh
$[Cr(Ph_2phen)_3](OTf)_3$	283 (103000); 307 (108000); 362 (35300), sh; 380 (26200), sh; 445 (2820), sh; 484 (1730), sh
$[Cr(bpy)_3](OTf)_3$	265 (15700); 275 (15500); 305 (21300), sh; 313 (23100); 346 (8100); 360 (5680), sh; 402 (950), sh; 428 (682), sh; 458 (291), sh
$[Cr(Me_2bpy)_3](OTf)_3$	278 (23100); 307 (25800); 342 (8530); 354 (6590), sh; 394 (892), sh; 418 (602), sh; 446 (256), sh
$[(phen)_2Cr(4\text{-}dmcbpy)](OTf)_3$ (**1**)	269 (50600); 285 (29900), sh; 329 (14300); 368 (5020), sh; 418 (1130), sh; 450 (634), sh; 480 (163), sh
$[(Ph_2phen)_2Cr(4\text{-}dmcbpy)](OTf)_3$ (**4**)	284 (63300); 311 (59300); 368 (21500), sh; 389 (11600), sh; 455 (1950), sh; 491 (1270), sh
$[(Me_2bpy)_2Cr(4\text{-}dmcbpy)](OTf)_3$ (**7**)	279 (23000), sh; 308 (21500); 333 (13500); 351 (9570), sh; 369 (4410), sh; 398 (1140), sh; 422 (866), sh; 451 (429), sh
$[Cr(4\text{-}dmcbpy)_3](BF_4)_3$ (**8**)	294 (14800), sh; 322 (20000), sh; 333 (22700); 360 (10500), sh; 372 (8210), sh; 420 (1280), sh; 448 (1020), sh; 480 (415), sh

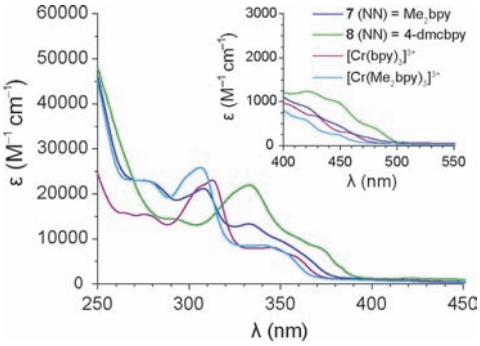

Figure 2. Electronic absorption spectra for Cr(III) dipyridyl complexes in 1 M $HCl_{(aq)}$ at room temperature.

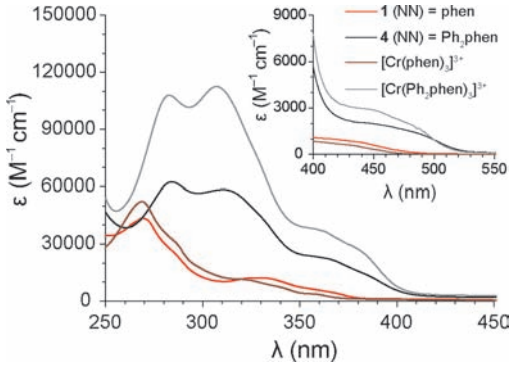

Figure 3. Electronic absorption spectra for Cr(III) complexes containing phenanthroline-based ligands: $[Cr(phen)_3]^{3+}$ and **1** in 1 M $HCl_{(aq)}$, $[Cr(Ph_2phen)_3]^{3+}$ and **4** in 1 M $HCl_{(aq)}$ with MeOH (2% v/v). All spectra were collected at room temperature.

As shown above, these complexes are strongly absorptive in the UV owing to ligand-centered $\pi \rightarrow \pi^*$ transitions; these are also observed in the free ligands. For $[Cr(bpy)_3]^{3+}$, $[Cr(Me_2bpy)_3]^{3+}$, and **7**, this includes the band in the vicinity of 300 nm. Ligand-centered $\pi \rightarrow \pi^*$ transitions due to the presence of 4-dmcbpy are seen red-shifted by ~10 nm in **7** and ~30 nm in **8**. For $[Cr(bpy)_3]^{3+}$, $[Cr(Me_2bpy)_3]^{3+}$, and **7**, the band in the vicinity of 350 nm appears to be charge transfer in nature based on its intensity and the fact that it is absent in the free ligand. A similar band is observed for **8** as a shoulder at ~375 nm. This red shift is consistent with expectations for metal-to-ligand charge-transfer (MLCT) given the presence of electron withdrawing substituents on the 4-dmcbpy ligands. However, one might also expect red shifting for ligand-to-metal charge transfer (LMCT) if such ligands serve to reduce electron−electron repulsion in the metal-centered orbitals. It is noted that the ~350 nm band in $[Cr(bpy)_3]^{3+}$ is most often attributed to LMCT[52,62,63] since there is an energetic penalty for oxidizing Cr(III) to Cr(IV) as would formally occur during MLCT.

For each of the bpy-containing complexes, a broad and modestly structured absorption feature is observed tailing into the visible spectrum (Figure 2 inset). Even for the known tris-homoleptic complexes $[Cr(bpy)_3]^{3+}$ and $[Cr(Me_2bpy)_3]^{3+}$, the observed molar absorptivities are larger than would be expected for pure spin-allowed ligand field transitions ($^4A_2 \rightarrow {}^4T_2$), and have been discussed in the literature.[52]

Here we accept that trigonal splitting is small (~20 cm^{-1})[64,65] and that these systems can be discussed with state designations normally reserved for systems with octahedral symmetry. The origin of this intensity enhancement is currently uncertain, but it has been claimed that spin−spin coupling between the ($^4A_2$) Cr(III) center and the triplet states of the aromatic ligand is a possible source.[52,66,67] Juban and McCusker have argued that visible absorption enhancement in $[Cr(bpy)_3]^{3+}$ is due to intensity borrowing from ligand-centered transitions.[68] This should be kept in mind as a possible mechanism in future explorations of 4-dmcbpy ligand-containing systems. It is noted here that for a Cr(III) species, $[Cr(4\text{-}dmcbpy)_3]^{3+}$ (**8**) shows appreciable sensitization of visible light, with a molar absorptivity of 940 M^{-1} cm^{-1} at 450 nm. This portends eventual control of this critical property through judicious structural and electronic modifications.

Figure 3 presents UV−visible absorption spectra for homo- and heteroleptic complexes containing phen-based ligands. Addition of 2% MeOH by volume to 1 M $HCl_{(aq)}$

(62) Milder, S. J.; Gold, J. S.; Kliger, D. S. *Inorg. Chem.* **1990**, *29*, 2506–2511.
(63) König, E.; Herzog, S. *J. Inorg. Nucl. Chem.* **1970**, *32*, 585–599.
(64) Hauser, A.; Maeder, M.; Robinson, W. T.; Murugesan, R.; Ferguson, J. *Inorg. Chem.* **1987**, *26*, 1331–1338.
(65) Schonherr, T.; Atanasov, M.; Hauser, A. *Inorg. Chem.* **1996**, *35*, 2077–2084.
(66) Ohno, T.; Kato, S.; Kaizaki, S.; Hanazaki, I. *Chem. Phys. Lett.* **1983**, *102*, 471–474.
(67) Ohno, T.; Kato, S.; Kaizaki, S.; Hanazaki, I. *Inorg. Chem.* **1986**, *25*, 3853–3858.
(68) Juban, E. A. Ph.D. Thesis, University of California, Berkeley, California, 2006.

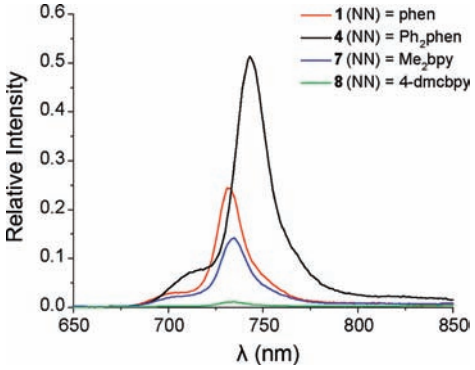

Figure 4. Emission spectra for Cr(III) polypyridyl complexes in deoxygenated 1 M $HCl_{(aq)}$ following excitation at 320 nm. On this intensity scale, the value 1 corresponds to the peak height in emission collected for $[Cr(phen)_3]^{3+}$.

was necessary to increase solubility for the Ph_2phen-containing complexes.[39]

Like the bipyridine-containing complexes discussed in Figure 2, intense ligand-centered $\pi \rightarrow \pi^*$ transitions are observed in the UV. For complexes with the unsubstituted phen ligand, this is most prominently observed at ~270 nm with very little shifting relative to the free ligand (264 nm for phen in CH_2Cl_2). Such transitions are significantly stronger and red-shifted in complexes containing the Ph_2phen ligand as evidenced by intense absorption bands at ~285 nm and ~310 nm. This is likely due to the presence of a larger and more delocalized π-system. For these two complexes, $[Cr(Ph_2phen)_3]^{3+}$ and **4**, new absorption features appear at ~375 nm upon formation of the metal complex. It is also noted that the intensity of the ~310 nm band mentioned above changes significantly relative to the free ligand where it appears as a shoulder to the bluer $\pi \rightarrow \pi^*$ band. We believe these substantive changes upon complexation herald charge transfer transitions (again, LMCT, MLCT, or both). For $[Cr(phen)_3]^{3+}$ and **1**, features absent in the free ligand spectra are observed at ~340 nm. The Ph_2phen-containing species **4** shows even more promising absorption of the visible spectrum than $[Cr(4\text{-dmcbpy})_3]^{3+}$ (**8**) discussed above: at 450 nm, $\varepsilon = 1960\ M^{-1}\ cm^{-1}$, and at 480 nm, $\varepsilon = 1490\ M^{-1}\ cm^{-1}$.

Static Emission. Each of the bis-heteroleptic polypyridyl Cr(III) complexes that we have synthesized (**1**, **4**, **7**, and **8**) is emissive at room temperature following electronic excitation. Emission spectra are shown in Figure 4 for dilute samples of the four ester-containing species in thoroughly deoxygenated 1 M $HCl_{(aq)}$ following excitation at 320 nm. The peaks of these spectra have been scaled to reflect relative intensity with respect to the nearly simultaneous measurement of a standard ($[Cr(phen)_3]^{3+}$ in thoroughly deoxygenated 1 M $HCl_{(aq)}$). We note that the wavelength of maximum emission at ~730 nm in **1**, **7**, and **8** is largely invariant to any changes made to the polypyridyl ligands. As shown in Table 3, the model homoleptic species $[Cr(phen)_3]^{3+}$, $[Cr(bpy)_3]^{3+}$, and $[Cr(Me_2bpy)_3]^{3+}$ emit most strongly at this approximate wavelength. Such emission λ_{max} invariance is common to Cr(III) polypyridyl species and indicates that the lowest energy excited state is insensitive to the ligand field, as would be the case for a ^2E state with a t_{2g}^3 configuration involving a spin flip.[45] By analogy to a large number of known emissive Cr(III) polypyridyl complexes, the main emission band seen at ~730 nm is assigned to the $^2E \rightarrow {}^4A$ (ground state) transition and the shoulder that occurs at ~700 nm is assigned to the $^2T \rightarrow {}^4A$ (ground state) transition.[39] Interestingly, and somewhat counter to the above discussion, Figure 4 and Table 3 show that the two species containing the Ph_2phen ligand, $[Cr(Ph_2phen)_3]^{3+}$ and $[(Ph_2phen)_2Cr(4\text{-dmcbpy})]^{3+}$ (**4**), have an emission λ_{max} that is shifted ~14 nm to the red. For $[Cr(Ph_2phen)_3]^{3+}$ this has also been reported elsewhere, although no explanation has been offered.[39] Electron delocalization via the larger π-system of the aryl-substituted ligand would reduce electron−electron repulsion in the t_{2g}^3 configuration of the ^2E state. However, a complete explanation of emission shifting must be more subtle as a similar reduction of repulsion in the t_{2g}^3 configuration of the ^4A ground state might be expected to cancel the effect in the excited state thereby leading to no shift in the emission maximum. One plausible explanation lies in the fact that doublet configurations involving spin pairing within individual metal orbitals contribute to the description of the emissive states in all of the these molecules explored herein, but for the aryl-substituted versions, the energetic perturbation due to these configurations is smaller as intraligand electronic delocalization takes effect.[69] Ultimately it will be important to determine whether there are connections between these emission shifting effects and the states playing roles in the absorption intensity borrowing (vide supra).

The emission spectra shown in Figure 4 allow us to determine the amount of energy stored in the long-lived excited states of these systems. This is a critical piece of information in assessing the oxidation potential available following absorption of UV−visible light. The values reported in Table 3 are for E_{00} (equivalent to the ΔG stored in the excited state) where we have modified the observed maximum of the 0−0 vibronic transition (E_0) with its width ($\Delta\bar{\nu}_{0,1/2}$) according to the expression

$$E_{00} = E_0 + (\Delta\bar{\nu}_{0,1/2})^2/16k_BT\ln 2 \qquad (2)$$

For emissive MLCT species (commonly, Ru^{II}, Os^{II}, and Re^{I}) one generally uses a Franck−Condon analysis to determine E_0 and $\Delta\bar{\nu}_{0,1/2}$.[70−72] Here, because emissive features from the $^2E \rightarrow {}^4A$ ground state are relatively narrow, we determine these quantities directly from the energy and width of the most intense band in the emission spectra.

We also report emission quantum yields in Table 3 for **1**, **4**, **7**, **8**, and our set of tris-homoleptic species relative to $[Cr(phen)_3]^{3+}$. The expression for the emission quantum yield ϕ_{em} in terms of radiative (k_r) and non-radiative (k_{nr}) rate constants is shown in eq 3. Here k_{obs} and τ_{obs} are inversely related and refer to the observed rate constant and lifetime, respectively.

$$\phi_{em} = \frac{\sum k_r}{\sum k_r + \sum k_{nr}} = \frac{\sum k_r}{k_{obs}} = \tau_{obs}\sum k_r \qquad (3)$$

If a comparison is drawn between $[Cr(phen)_3]^{3+}$ and $[(phen)_2Cr(4\text{-dmcbpy})]^{3+}$ (**1**), it is seen that introduction of a single 4-dmcbpy ligand drops the quantum yield to 28% of its value in the homoleptic species. For the

(69) Kirk, A. D. *Chem. Rev.* **1999**, *99*, 1607–1640.
(70) Claude, J. P.; Meyer, T. J. *J. Phys. Chem.* **1995**, *99*, 51–54.
(71) Kober, E. M.; Caspar, J. V.; Lumpkin, R. S.; Meyer, T. J. *J. Phys. Chem.* **1986**, *90*, 3722–3734.
(72) Chen, P. Y.; Meyer, T. J. *Chem. Rev.* **1998**, *98*, 1439–1477.

Table 3. Photophysical Data for Cr(III) Polypyridyl Complexes in 1 M $HCl_{(aq)}$

complex	emission[a] λ_{max} /nm	E_{00}[b] / eV	normalized emission quantum yield[a,c,d]	emission quantum yield[a,e] $\times 10^3$	emission lifetime[a,c] /μs	ln(A)[f]	A /s^{-1}	E_a[f] / kJ·mol^{-1}
$[Cr(phen)_3](OTf)_3$	730	1.70	1	12 ± 1[c]	304 ± 4	28.9 ± 0.5	3.5×10^{12}	51 ± 1
$[Cr(Ph_2phen)_3](OTf)_3$	744	1.67	2.5 ± 0.4	30 ± 5[g]	425 ± 20	26 ± 1	2.4×10^{11}	45 ± 3
$[Cr(bpy)_3](OTf)_3$	729	1.71	0.21 ± 0.01	2.5 ± 0.2[g]	69 ± 2	27.0 ± 0.3	5.5×10^{11}	43 ± 1
$[Cr(Me_2bpy)_3](OTf)_3$	732	1.70	0.74 ± 0.03	8.9 ± 0.9[g]	196 ± 8	28.5 ± 0.5	2.3×10^{12}	49 ± 1
$[(phen)_2Cr(4\text{-}dmcbpy)](OTf)_3$ (**1**)	732	1.70	0.28 ± 0.01	3.4 ± 0.4[g]	87 ± 3	27.8 ± 0.5	1.2×10^{12}	46 ± 1
$[(Ph_2phen)_2Cr(4\text{-}dmcbpy)](OTf)_3$ (**4**)	742	1.68	0.55 ± 0.02	6.6 ± 0.7[g]	108 ± 8	27.3 ± 0.5	7.5×10^{11}	45 ± 1
$[(Me_2bpy)_2Cr(4\text{-}dmcbpy)](OTf)_3$ (**7**)	734	1.70	0.15 ± 0.01	1.8 ± 0.2[g]	47 ± 1	28.6 ± 0.2	2.6×10^{12}	46 ± 1
$[Cr(4\text{-}dmcbpy)_3](BF_4)_3$ (**8**)	733	1.70	0.012 ± 0.002	0.14 ± 0.02[g]	7.7 ± 0.3	26.7 ± 0.4	4.1×10^{11}	37 ± 1

[a] The measurements were done at 23−24 °C. [b] See text for details on the calculation of E_{00}. [c] The errors represent 2σ (two times of standard deviation) from nine measurements (three independent experiments for each sample, three measurements for each experiment.) [d] The normalized emission quantum yields were determined with respect to $[Cr(phen)_3]^{3+}$. [e] Emission quantum yields reported are relative to the standard $[Ru(bpy)_3]^{2+}$ in acetonitrile with a 0.062 absolute emission quantum yield. See Experimental Section for details. [f] Errors reported reflect 2σ from the fitting of a single temperature-data set to a linear Arrhenius model $\ln k_{obs} = \ln A - E_a/RT$. [g] See Experimental Section for details on the calculation of these error bars.

comparisons between $[Cr(Me_2bpy)_3]^{3+}$ and $[(Me_2bpy)_2Cr(4\text{-}dmcbpy)]^{3+}$ (**7**) or between $[Cr(Ph_2phen)_3]^{3+}$ and $[(Ph_2phen)_2Cr(4\text{-}dmcbpy)]^{3+}$ (**4**), these values are 21% and 21.5%, respectively. In the comparison between $[Cr(bpy)_3]^{3+}$ and $[Cr(4\text{-}dmcbpy)_3]^{3+}$(**8**), introduction of three 4-dmcbpy ligands in place of the three bpy ligands drops the quantum yield to ~6% of the value prior to the substitution. The origin of these quantum yield changes is discussed below.

Time-Resolved Emission. To understand these trends in radiative quantum yields, we have measured the observed lifetimes (τ_{obs}) of the emissive ^2E states in the full set of complexes and these are also reported in Table 3. For the new complexes reported here, the lowest energy excited state lifetimes range from 108 μs (for **4**) to 7.7 μs (for **8**). This is encouraging as it suggests there may be ample time in the ^2E excited-state of the respective complexes to engage in hole transfer photochemistry. In the comparison between $[Cr(phen)_3]^{3+}$ and $[(phen)_2Cr(4\text{-}dmcbpy)]^{3+}$ (**1**), the observed lifetime drops from 304 to 87 μs upon introduction of the 4-dmcbpy ligand. This latter value is 29% of that measured for the tris-homoleptic species. Similar comparisons made between $[Cr(Me_2bpy)_3]^{3+}$ and $[(Me_2bpy)_2Cr(4\text{-}dmcbpy)]^{3+}$ (**7**) or between $[Cr(Ph_2phen)_3]^{3+}$ and $[(Ph_2phen)_2Cr(4\text{-}dmcbpy)]^{3+}$ (**4**) yield the values 24% and 25%, respectively. The comparison between $[Cr(bpy)_3]^{3+}$ and $[Cr(4\text{-}dmcbpy)_3]^{3+}$(**8**) shows that introduction of a full set of ester-containing ligands drops the observed lifetime (7.7 μs) to 11% of the value obtained for $[Cr(bpy)_3]^{3+}$ (69 μs). The various percentage changes in τ_{obs} shown here are similar to those seen above for ϕ_{em}. This correspondence suggests (by eq 3) that introduction of the 4-dmcbpy ligand mainly affects the rate constants for non-radiative relaxation pathways ($\sum k_{nr}$).

To better understand the origin of the lifetime drop for **8**, we have explored the temperature dependence of emission lifetimes for the complete series of complexes over the range 283 K−353 K. A representative example is shown in Figure 5 for **8** compared to $[Cr(bpy)_3]^{3+}$ as the natural log of the observed rate constant (k_{obs}) versus 1000/T. Other data sets for the remaining compounds are shown in the Supporting Information, Figure S3.

In all cases we observe temperature dependence. The high-degree of linearity for all data sets suggests that in this temperature range (throughout which we have a fluid solution) the activated process dominates the observed

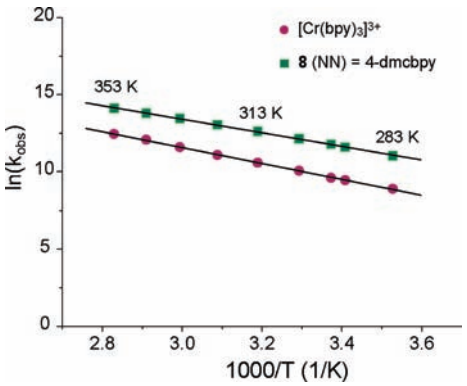

Figure 5. Temperature dependence of the observed rate constant $k_{obs} = 1/\tau_{obs}$ for $[Cr(bpy)_3]^{3+}$ and **8** in degassed 1 M $HCl_{(aq)}$.

rate constant relative to temperature-independent contributions to k_r and k_{nr}.[73] Table 3 includes a listing of the measured Arrhenius pre-exponential (A) and activation energy (E_a) for each system. With this information we can see general trends emerge, especially if we draw comparisons, as before, between pairs of compounds where ancillary ligands are the same. For example in comparing $[Cr(phen)_3]^{3+}$ and **1** it is seen that introduction of the ester-containing ligand serves to drop the activation energy by 5 kJ/mol. Given that the pre-exponential A drops modestly between $[Cr(phen)_3]^{3+}$ and **1**, the concomitant decrease in E_a is responsible for the shortening of the lifetime from 304 to 87 μs. A similar decrease in E_a is also observed between $[Cr(Me_2bpy)_3]^{3+}$ and **7** and the system with shortest lifetime, **8**, also has the smallest E_a which is 6 kJ/mol less than that measured for $[Cr(bpy)_3]^{3+}$. These observations can be explained if introduction of the electron withdrawing ester ligand weakens the ligand field via an inductive effect, thereby decreasing the barrier to excited states having a $t_{2g}{}^2e_g$ configuration. Such states would have significant nuclear distortions (primarily metal−ligand bond distances) and through these displacements larger non-radiative decay rates. Given the magnitude of the Arrhenius pre-exponential A measured for these systems, it is unlikely that these complexes are thermally activated directly through back-intersystem-crossing from the ^2E to the ^4T manifold. Rather one might need to invoke deactivation through states with appropriate nuclear distortion but also with doublet electron spin character. It is noted that differences

(73) Forster, L. S. *Coord. Chem. Rev.* **2002**, *227*, 59–92.

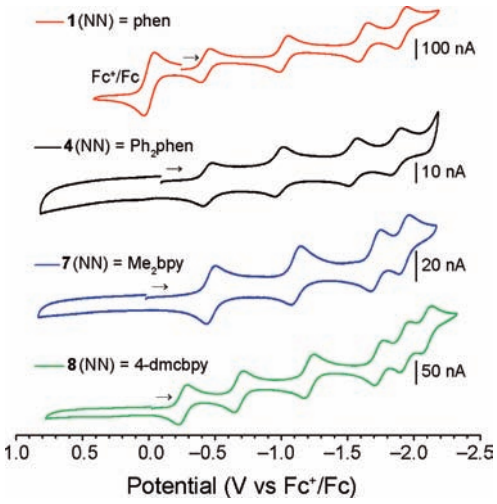

Figure 6. Comparison of cyclic voltammograms for the 4-dmcbpy containing complexes **1**, **4**, **7**, and **8** in 0.1 M $TBAPF_6$ acetonitrile solution. Arrows indicate the starting point and direction for each voltammogram. For **4**, **7**, and **8**, the potential is referenced to ferrocene (from a voltammogram which includes Fc collected immediately after the displayed voltammogram).

in activation energy alone are not sufficient to explain the significant lifetime variation between $[(Ph_2phen)_2Cr(4\text{-}dmcbpy)]^{3+}$ (**4**) where $\tau_{obs} = 108\ \mu s$, and $[Cr(Ph_2phen)_3]^{3+}$ where $\tau_{obs} = 425\ \mu s$. Here, differences in the Arrhenius preexponential A are the primary origin of the observation. It does not appear to be simply a consequence of the reduced rigidity of the diester ligand and related entropic effects as we do not see A increase between $[Cr(phen)_3]^{3+}$ and $[(phen)_2Cr(4\text{-}dmcbpy)]^{3+}$ (**1**). Detailed theoretical exploration is needed to determine, for example, whether there are changes in the density of electronic states at the activation energy of ~45 kJ/mol in the comparison between $[Cr(Ph_2phen)_3]^{3+}$ and $[(Ph_2phen)_2Cr(4\text{-}dmcbpy)]^{3+}$ (**4**) that might influence the relative mechanisms for non-radiative decay.

Ground and Excited State Reduction Potentials. Along with emission data, the second critical component for finding excited state redox potentials is the determination of ground state "$Cr^{III/II}$" and "$Cr^{IV/III}$" couples. Each of the heteroleptic dipyridyl complexes **1**, **4**, and **7** show 4 reversible $1e^-$ reductions, and in the case of **8**, six reversible waves are seen. The "$Cr^{IV/III}$" couples for these systems have not been observed as they are outside of the acetonitrile solvent oxidation window. These data are presented here in Figure 6 and Table 4.

As shown, the first reduction for complexes containing the ester ligands is facile, with $E_{1/2}$ occurring between −0.47 and −0.42 V versus Fc^+/Fc for all species containing a single ester ligand. We find that the position of the first wave can be tuned through the functional groups present on the attached ligands. The presence of two strongly electron withdrawing ester groups on the ligand 4-dmcbpy shifts the initial "$Cr^{III/II}$" process to more positive potentials compared to those previously reported for hetero- and homoleptic $[Cr(NN)_3]^{3+}$ complexes.[49,57] This is shown in Table 4: for **1**, **4**, and **7**, the first "$Cr^{III/II}$" reduction occurs at a potential at least 0.22 V more positive than the homoleptic species that lack an ester ligand. For $[Cr(4\text{-}dmcbpy)_3]^{3+}$ (**8**) this first reduction is remarkably shifted an additional ~0.2 V in the positive direction compared to the complexes containing a single 4-dmcbpy. For this species the presence of three ligands carrying electron withdrawing groups is able to move the "$Cr^{-I/-II}$" and "$Cr^{-II/-III}$" reductions to within the acetonitrile window, leading to the observation of six reversible waves. While each of these reductions is listed as a change in the Cr formal oxidation state (matching the literature precedent), these processes are more likely due to ligand reduction,[63,74,75] and it is reasonable to surmise that the presence of electron withdrawing groups allow for each 4-dmcbpy ligand to be reduced by two electrons.

The half wave reduction potential of the excited state can be estimated using the ground state half wave reduction potential and the one electron potential corresponding to the spectroscopic excited state:[76]

$$E_{1/2}(Cr^{III*/II}) = E_{00}(Cr^{III*/III}) + E_{1/2}(Cr^{III/II}) \qquad (4)$$

The use of E_{00} as a potential (rather than energy) is acceptable in this context because the excited state is only acting as a one-electron acceptor. As discussed in the context of Table 3, E_{00} is largely invariant to ligand substitution patterns. Others have noted that the ^2E emission maximum in Cr(III) species is solvent insensitive, and we have observed that E_{00} does not change between aqueous (where our spectroscopic measurements have been made) and acetonitrile (where our electrochemical measurements have been made) environments. On the other hand, the ground state (first) reduction potentials show ligand dependence (Table 4). Thus, the excited state reduction potential is tunable. These values are compiled in Table 4 for all the complexes studied. Equation 4 allows us to predict a $Cr^{III*/II}$ couple of +1.22 to +1.27 V versus Fc^+/Fc for the heteroleptic complexes. To compare the excited state potentials of these Cr(III) complexes to other photoelectrochemically active species reported in the literature, the measured redox potentials have been converted to reference NHE (Fc^+/Fc is 0.40 V vs SCE in 0.1 M $TBAPF_6$[77] and SCE is 0.241 V vs NHE[78]). We note that this comparison is approximate because of differences in solvent and supporting electrolyte, but it is still useful.[79] In the case of **8**, the $Cr^{III*/II}$ couple is calculated to be a remarkable +2.08 V versus NHE while **1**, **4**, and **7** are +1.92 V, +1.87 V, and +1.87 V versus NHE, respectively. As a point of reference, a similar ester-functionalized $[Ru(NN)_3]^{2+}$ complex shows an excited state reduction potential of +1.26 V (vs NHE) for $Ru^{II*/I}$.[80] Reece and Nocera reported +1.78 V (vs NHE) for a $Re^{I*/0}$ complex,[81] while Sullivan and co-workers reported +2.71 V (vs NHE) for a $Re^{II*/I}$ complex.[82] Reports of $Cr^{III*/II}$ potentials from non-polypyridyl complexes are very rare in the literature; however, an amine based $Cr^{III*/II}$ system has been reported with an excited state reduction potential of

(74) Saito, Y.; Takemoto, J.; Hutchinson, B.; Nakamoto, K. *Inorg. Chem.* **1972**, *11*, 2003–2011.
(75) Creutz, C. *Comments Inorg. Chem.* **1982**, *1*, 293–311.
(76) Ballardini, R.; Varani, G.; Indelli, M. T.; Scandola, F.; Balzani, V. *J. Am. Chem. Soc.* **1978**, *100*, 7219–7223.
(77) Connelly, N. G.; Geiger, W. E. *Chem. Rev.* **1996**, *96*, 877–910.
(78) Bard, A. J.; Faulkner, L. R. *Electrochemical methods fundamentals and applications*, 2nd ed.; Wiley: New York, 2001.
(79) Pavlishchuk, V. V.; Addison, A. W. *Inorg. Chim. Acta* **2000**, *298*, 97–102.
(80) Monserrat, K.; Foreman, T. K.; Grätzel, M.; Whitten, D. G. *J. Am. Chem. Soc.* **1981**, *103*, 6667–6672.
(81) Reece, S. Y.; Nocera, D. G. *J. Am. Chem. Soc.* **2005**, *127*, 9448–9458.
(82) Del Negro, A. S.; Seliskar, C. J.; Heineman, W. R.; Hightower, S. E.; Bryan, S. A.; Sullivan, B. P. *J. Am. Chem. Soc.* **2006**, *128*, 16494–16495.

Table 4. Ground and Excited State Reduction Potentials for Cr(III) Polypyridyl Complexes

	($E_{1/2}$ vs Fc^+/Fc, V)[a]						
	3+/2+	2+/1+	1+/0	0/1−	1−/2−	2−/3−	*3+/2+ [b]
$[Cr(phen)_3](OTf)_3$	−0.65	−1.17	−1.71	−2.21			+1.05
$[Cr(Ph_2phen)_3](OTf)_3$	−0.67	−1.11	−1.63	−2.05			+1.00
$[Cr(bpy)_3](OTf)_3$	−0.63	−1.15	−1.72	−2.34			+1.08
$[Cr(Me_2bpy)_3](OTf)_3$	−0.79	−1.29	−1.82				+0.91
$[(phen)_2Cr(4\text{-dmcbpy})](OTf)_3$ (**1**)	−0.42	−1.01	−1.61	−1.90			+1.28
$[(Ph_2phen)_2Cr(4\text{-dmcbpy})](OTf)_3$ (**4**)	−0.45	−0.99	−1.54	−1.87			+1.23
$[(Me_2bpy)_2Cr(4\text{-dmcbpy})](OTf)_3$ (**7**)	−0.47	−1.11	−1.71	−1.92			+1.23
$[Cr(4\text{-dmcbpy})_3](BF_4)_3$ (**8**)	−0.26	−0.68	−1.21	−1.74	−1.93	−2.10	+1.44

[a] Conditions for cyclic voltammetry of Cr complexes: electrolyte, 0.1 M $TBAPF_6$ in CH_3CN; WE, Pt; CE, Pt Wire; scan rate, 100 mV/s. [b] Calculated from eq 4.

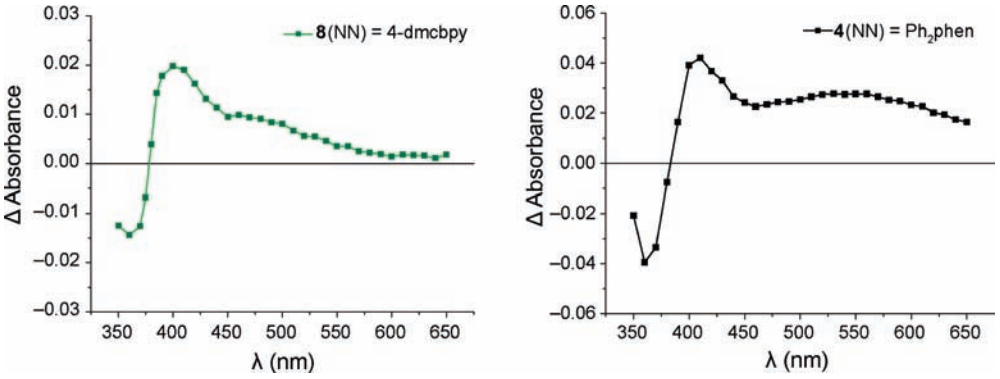

Figure 7. Transient absorption spectra on a microsecond time scale for **8** (left) and **4** (right) in 1 M $HCl_{(aq)}$. The spectra were determined from a single exponential fit to transient absorption (or bleach) kinetics collected at each of the wavelengths for which there is a dot. The lines are included as guides to the eye.

+0.77 V (vs NHE).[83] Indeed, the ester-containing Cr(III) complexes **1**, **4**, **7**, and **8** offer themselves as potentially powerful excited state oxidants.

Transient Absorption. In future studies involving hole transfer photochemistry between Cr(III) systems and wide band gap semiconductors to which they are bound, it will be important to be able to interrogate the time-dependent behavior of the lowest energy excited-state manifold in these complexes without relying on emission and on potentially very short time scales. A valuable tool in this context is transient electronic absorption (TA) spectroscopy. With time resolution from tens of femtoseconds to milliseconds, TA spectroscopy has been central to unraveling the mechanism in dye-sensitized heterojunction solar cell materials.[6,7,84] Here we do not consider the earliest transient events but rather explore absorption features once these molecules are electronically relaxed in the ^2E excited states. The spectrometer used here employs ~10 ns excitation pulses centered at 355 nm and the transient features probed with white light decay with single exponential behavior on microsecond time scales. Within such time scales, it is well established that the ^2E excited-state of these complexes in fluid solution at room temperature is vibrationally cool and thermally equilibrated with the solvent.[68,69,85−91] TA spectra collected for the tris-homoleptic compounds $[Cr(phen)_3]^{3+}$, $[Cr(bpy)_3]^{3+}$, $[Cr(Me_2bpy)_3]^{3+}$, and $[Cr(Ph_2phen)_3]^{3+}$ are shown in Supporting Information, Figure S2, and these agree with previously reported spectra collected under similar experimental conditions.[39] Spectra for the two additional bis-heteroleptic complexes **1** and **7** are also shown in the Supporting Information, Figure S2. In the case of **7**, the spectrum is quite similar to that of the related tris-homoleptic species $[Cr(Me_2bpy)_3]^{3+}$. There are some qualitative differences between **1** and $[Cr(phen)_3]^{3+}$ in terms of relative band intensities, but these are unremarkable and are not considered here further. In Figure 7 are plotted transient absorption (TA) spectra for **8** (left) and **4** (right). As discussed above, these species have the most promising molar absorptivities of visible wavelengths and are likely, therefore, to be used in future semiconductor sensitization experiments.

Both difference spectra show a resolved bleach feature centered at 360 nm, a strong absorption feature at ~400 nm, and a broad absorption further to the red. In the case of **4**, this redder absorbance is very broad and appears to peak at ~550 nm. The magnitude of the bleach in both transient spectra provides a useful metric for estimating excited-state molar absorptivities at various wavelengths. In the ground state optical spectra shown in Figure 2 and Figure 3, complexes **8** and **4** exhibit molar extinction coefficients at 360 nm of $\varepsilon_{360\ nm} = 10500\ M^{-1}\ cm^{-1}$ and $\varepsilon_{360\ nm} = 23400\ M^{-1}\ cm^{-1}$, respectively. In the limiting case that the $-\Delta A$ at 360 nm for

(83) Ramasami, T.; Endicott, J. F.; Brubaker, G. R. *J. Phys. Chem.* **1983**, *87*, 5057–5059.
(84) Grätzel, M. *Inorg. Chem.* **2005**, *44*, 6841–6851.
(85) Serpone, N.; Jamieson, M. A.; Hoffman, M. Z. *J. Chem. Soc., Chem. Commun.* **1980**, 1006–1007.
(86) Serpone, N.; Jamieson, M. A.; Sharma, D. K.; Danesh, R.; Bolletta, F.; Hoffman, M. Z. *Chem. Phys. Lett.* **1984**, *104*, 87–92.
(87) Kirk, A. D.; Porter, G. B.; Sharma, D. K. *Chem. Phys. Lett.* **1986**, *123*, 548–550.
(88) Serpone, N.; Hoffman, M. Z. *Chem. Phys. Lett.* **1986**, *123*, 551–552.
(89) Rojas, G. E.; Dupuy, C.; Sexton, D. A.; Magde, D. *J. Phys. Chem.* **1986**, *90*, 87–92.
(90) Rojas, G. E.; Magde, D. *J. Phys. Chem.* **1987**, *91*, 689–691.
(91) Serpone, N.; Hoffman, M. Z. *J. Phys. Chem.* **1987**, *91*, 1737–1743.

these two spectra is entirely due to loss of ground state absorption, then it is possible to assign a lower limit to excited-state molar absorptivities ($\varepsilon^*_{(\lambda)}$) for observed absorption features. In the case of **8**, we measure $\Delta A = -0.014$ at 360 nm and $\Delta A = 0.020$ at 400 nm such that $\varepsilon^*_{400\ nm} \geq 14400\ M^{-1}\ cm^{-1}$. A similar observation is made for **4** although the absorptivities are even larger. In this case $\varepsilon^*_{400\ nm} \geq 23300\ M^{-1}\ cm^{-1}$ and $\varepsilon^*_{550\ nm} \geq 16500\ M^{-1}\ cm^{-1}$. In these spectra (and very likely in the whole series of Cr(III) polypyridyl complexes we have considered), the transient absorption features with appreciable ΔA are clearly not assignable to ligand-field absorption occurring from the t_{2g}^3 configuration of the ^2E excited state. The strength of the absorption features suggest these are charge transfer in nature originating from the ^2E and ^2T excited states, although it is not possible at this time to assign MLCT and/or LMCT to any particular feature. The t_{2g}^3 configuration of the ^2E excited state is not expected to significantly perturb the ligand π-system, so ligand-centered $\pi \rightarrow \pi^*$ transitions are unlikely to play a prominent role. It may be possible that the observed transitions, especially those near 400 nm, borrow some intensity from such excitations as Juban and McCusker[68] have argued occurs in the ground state of $[Cr(bpy)_3]^{3+}$. The important point to stress here is that excited-state absorption features in the visible spectrum for these complexes have significant oscillator strength. In more complex environments such as when complexes are bound to heterogeneous semiconductor surfaces, such features may be a useful and easily observable diagnostic of ^2E lifetime and related hole-injection rate constants.

Conclusions and Outlook

The preparation of heteroleptic dipyridyl Cr(III) complexes that contain at least one carboxylate group (for eventual attachment to semiconductor surfaces) was not known prior to our efforts. We have synthesized four such complexes, including three heteroleptic $[(NN)_2Cr(4\text{-dmcbpy})]^{3+}$ species. We have also explored the basic photophysical and electrochemical properties of these systems to better understand the nascent and long-lived excited-states that will be called upon to drive hole-injection following photoexcitation in later studies.

The electronic absorption studies show a combination of ligand-centered, metal-centered ligand field, and charge transfer transitions. Nevertheless, it is noted here that for a Cr(III) species with Ph_2phen ancillary ligands, $[(Ph_2phen)_2Cr(4\text{-dmcbpy})]^{3+}$ (in **4**), shows appreciable sensitization of visible light, with a molar absorptivity of 1270 $M^{-1}\ cm^{-1}$ at 491 nm. Time-resolved emission studies show that the introduction of the 4-dmcbpy ligand decreases the doublet excited state lifetimes of the complexes with respect to their tris-homoleptic analogues. Notwithstanding, excited state lifetimes are sufficiently long that we can anticipate photoinduced hole transfer to suitable semiconductor substrates. Additionally, preliminary electrochemical studies show that the introduction of the 4-dmcbpy significantly shifts reduction potentials of the complexes to more positive values. The combination of cyclic voltammetry and static emission studies indicates that strongly oxidizing excited states are possessed by this class of molecules.

The strongly oxidizing excited states found for the Cr(III) dye complexes coupled with the reported long excited state lifetimes lead us to believe these species will be capable of hole injection into p-type semiconductors with suitably aligned valence bands. Further, the excited-state absorption features for these heteroleptic complexes should serve as handles for studying the hybrid dye-sensitized materials. Efforts are underway to incorporate these dye complexes with semiconductors into hybrid materials.

Acknowledgment. This research was supported by Honda (2008 Honda Initiation Grant), the Center for Revolutionary Solar Photoconversion, Colorado State University, and the University of Colorado. We thank Prof. C. M. Elliott and Prof. C. Koval for helpful discussions and Dr. Md. K. Kabir for initial efforts on preparing $[Cr(dcbpy)_n]^{x+}$ complexes.

Supporting Information Available: X-ray structural data (cif); details of spectroscopic and electrochemical characterizations (pdf). This material is available free of charge via the Internet at http://pubs.acs.org.